entropy

MDPI

Article

Isothermal Oxidation of Aluminized Coatings on High-Entropy Alloys

Che-Wei Tsai [1,*], Kuen-Cheng Sung [1], Kzauki Kasai [2] and Hideyuki Murakami [2]

[1] Department of Materials Science and Engineering, National Tsing Hua University, Hsinchu 30013, Taiwan; df8805566@yahoo.com.tw

[2] Surface and Interface Kinetics Group, National Institute for Materials Science, Sengen 1-2-1, Tsukuba, Ibaraki 305-0047, Japan; kazuki_87286@docomo.ne.jp (K.K.); MURAKAMI.Hideyuki@nims.go.jp (H.M.)

* Correspondence: chewei@mx.nthu.edu.tw; Tel.: +886-3-571-5131 (ext. 35370)

Academic Editor: Kevin H. Knuth

Received: 31 July 2016; Accepted: 14 October 2016; Published: 20 October 2016

Abstract: The isothermal oxidation resistance of $Al_{0.2}Co_{1.5}CrFeNi_{1.5}Ti_{0.3}$ high-entropy alloy is analyzed and the microstructural evolution of the oxide layer is studied. The limited aluminum, about 3.6 at %, leads to the non-continuous alumina. The present alloy is insufficient for severe circumstances only due to chromium oxide that is 10 μm after 1173 K for 360 h. Thus, the aluminized high-entropy alloys (HEAs) are further prepared by the industrial packing cementation process at 1273 K and 1323 K. The aluminizing coating is 50 μm at 1273 K after 5 h. The coating growth is controlled by the diffusion of aluminum. The interdiffusion zone reveals two regions that are the Ti-, Co-, Ni-rich area and the Fe-, Cr-rich area. The oxidation resistance of aluminizing HEA improves outstandingly, and sustains at 1173 K and 1273 K for 441 h without any spallation. The alumina at the surface and the stable interface contribute to the performance of this $Al_{0.2}Co_{1.5}CrFeNi_{1.5}Ti_{0.3}$ alloy.

Keywords: high entropy alloys; aluminizing; isothermal oxidation

1. Introduction

High-entropy alloys (HEAs) were brought forward two decades ago by Professor Yeh's group. The brief concept and outcomes are discussed on specific microstructures, with resistance to annealing softening and outstanding mechanical properties at high temperature, in the first paper in 2004 [1]. The excellent performance of HEAs is contributed to by the four core effects, and they are the high-entropy effect, the lattice-distortion effect, the sluggish effect, and the cocktail effect [2]. The HEAs provide countless compositions to study their physical phenomena and structural properties for functional uses. More and more researchers study the phenomena in different HEAs systems.

The equiatomic multicomponent AlCoCrFeNiTi high-entropy solid solution alloy has been fabricated by vacuum arc melting and studied on the effect of the aluminum molar ratio. It reveals that only a face-centered cubic crystal structure phase is observed in the CoCrFeNiTi alloy. The phase composition transforms to stabilized body-centered cubic structure phases when Al is added [3]. The alloy is also synthesized by mechanical alloying with a high-energy planetary ball mill. Two solid solution phases, supersaturated BCC (body center cubic) and FCC (face center cubic), appear when the blended powder is ball milled more than 18 h [4]. The AlCoCrFeNiTi high-entropy alloy contains more intermetallic compounds after annealing treatment, and there are many compounds, including $CoTi_2$ and FeTi, in CoCrFeNiTi alloy even without aluminum [5,6]. Above all, it means the aluminum is a strong BCC former. The molar ratio of titanium also needs to be reduced to avoid compounds.

The non-equiatomic multicomponent $Al_xCo_{1.5}CrFeNi_{1.5}Ti_y$ (x = 0 and 0.2, y = 0.5 and 1) had been investigated systematically by our group [7]. The amount of Al and Ti affect the formation of hard eta phase $(Ni, Co)_3Ti$, although it enhances the two-times-higher wear resistance of HEAs than

SUJ2 and SKH51 at the same hardness. The SUJ2 bearing steel and SKH51 high-speed steel have good mechanical properties and are proven anti-wear alloys. However, the workability and ductility of $Al_xCo_{1.5}CrFeNi_{1.5}Ti_y$ needs to be improved for application, so the lower molar ratio of Al and Ti, x + y = 0.5, is studied. As y > 0.4, the eta phase still can be observed at 900 °C or 1000 °C for 50 h. In the isothermal oxidation test at 900 °C, the continuous Cr_2O_3 is formed on the surface for protection, but it is still limited for application compared with the superalloy Inconel 718 [8,9]. Inconel 718 is a known chromia former, and has the best oxidation resistance compared to other alloys until now. At x < 0.2, a lower Al molar ratio is insufficient for oxidation resistance.

Increasing the Al ratio generally results in forming a BCC solid solution phase in HEAs. The HEAs with a BCC phase generally have low workability and ductility at ambient temperature. Therefore, forming aluminum-rich coatings, built up by a diffusion zone, can protect the surface against oxidation. That is the method for HEAs to confront temperature up to 1400 K and even higher. The same matter is also resolved for superalloys, since they are widely used for blades in turbine engines [10–13]. In aircraft, the gas turbines have been equipped with single-crystal blades. The aluminizing process is an effective coating method frequently used for the protection of metal surfaces against oxidation, via the formation of an α-Al_2O_3 layer. This technique is provided with a simple apparatus set-up, high cost performance and uniform formation of coatings [12–14].

In this paper, the FCC phase of $Al_{0.2}Co_{1.5}CrFeNi_{1.5}Ti_{0.3}$ HEA is studied. The isothermal oxidation resistance of HEA and aluminizing HEA are analyzed after for various times at 1173 K and 1273 K. Since the continuous and dense alumina is not formed at the surface, the present alloys are poorly oxidation resistant according to the literature. The evolution of oxide layers is shown in the isothermal testing of HEAs, and the microstructures and distributed region are further discussed. This is the first finding that HEAs are suitable for industrial aluminization. For the aluminizing coating on HEAs, the oxidation resistance is improved and its sustaining temperature is increased up to 1273 K.

2. Materials and Methods

The $Al_{0.2}Co_{1.5}CrFeNi_{1.5}Ti_{0.3}$ HEA ingots were prepared from the mixtures of the constituent elements with purities higher than 99.5 wt % in an argon atmosphere, and the melting procedure was repeated five times to improve the homogeneity of the ingots by arc-melting. The dimension of slab is 40 × 20 mm with 10 mm in thickness, and further homogenized at 1100 °C for 6 h with water quenching in air. After that, it is rolled to 3 mm at ambient temperature with 70% thickness reduction. The plate was machining by electrical discharge machining machine. The samples with 10 mm in diameter are used for isothermal oxidation test, and another with 9 mm in square are for aluminization.

For the aluminization, the specimens were embedded in a heat-resistant container with a powder mixture of 24.5 wt % Al (45–106 μm in size), 24.5 wt % Cr (45 μm in size), 49.0 wt % Al_2O_3 (15–63 μm in size) and 2.0 wt % NH_4Cl. This container was placed in a vacuum furnace that was evacuated down to 1.0×10^{-1} Pa at ambient temperature using a rotary mechanical pump. After the furnace was evacuated, Ar was introduced until the pressure reached 1.0×10^5 Pa (1 atm). This process of evacuation and flushing with Ar was repeated three times. Two heating processes, 1273 K and 1323 K, are used respectively. The furnace was heated at a rate of 10 K/min and kept at the temperature for 5 h while Ar was flowed through the furnace at a rate of 200 mL/min.

In the isothermal heating test, the specimens of HEAs and aluminized HEAs were kept heated at 1173 K, 1273 K and 1373 K for different endurance time from 1 h to 441 h. All specimen surfaces were grinded before oxidation test and aluminizing process. The oxidation weight gains of specimens were measured by digital weighing scale, and cross-sections were examined. The specimens were prepared by the process of mounting, grinding and polishing. Scanning electron microscopy (SEM, JEOL JSM-6010, JEOL Ltd., Tokyo, Japan) equipped with energy dispersive X-ray spectrometry (EDS, Oxford Instruments, Oxfordshire, UK) is applied to observe and analyze the microstructure and composition of oxide layers. The oxides are identified by an X-ray diffractometer (XRD, RINT2500,

Rigaku, Tokyo, Japan) with Cu-target radiation. The specimens are analyzed at 2θ angles from 20° to 100° with a scanning rate of 2 deg./min.

3. Results

3.1. Isothermal Oxidation of HEA without Aluminizing Coating

The $Al_{0.2}Co_{1.5}CrFeNi_{1.5}Ti_{0.3}$ HEA contains aluminum and chromium, and the amount of both is about 21.8 at %. It is well known that it forms alumina and chromium oxide to protect the alloys generally. However, the weight gain of oxidation at 1173 K and 1273 K was shown to be poor in Figure 1. At 1173 K the curve is similar to that found in the previous literature [9]. That oxidation layer will detach from the substrate and the weight gain decreases after 100 h. Under only 1273 K for 50 h, the layer detaches from the substrate, and the spallation is more serious than that at 1173 K. Figure 1a shows the surface morphology of samples at 1273 K for 180 h. Thus, the weight gains of the present alloys decrease drastically, because the oxide layers are spalled both at the top side or the bottom side.

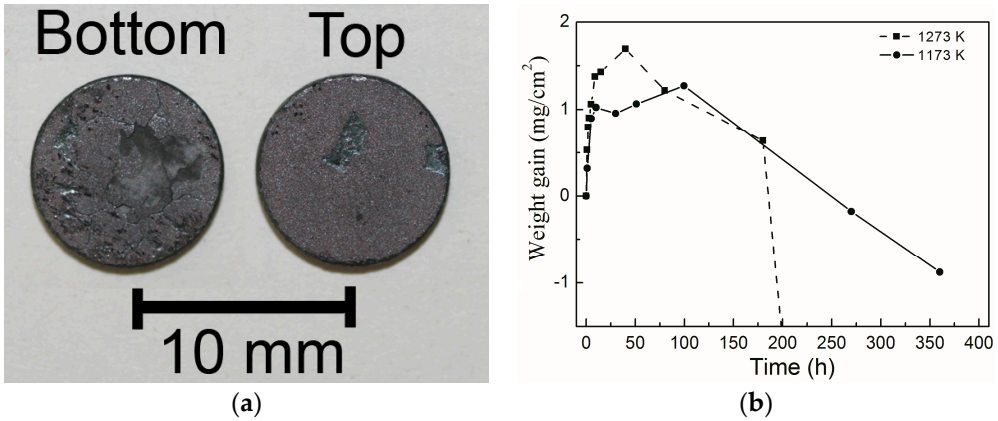

Figure 1. The isothermal oxidation of $Al_{0.2}Co_{1.5}CrFeNi_{1.5}Ti_{0.3}$ alloys: (**a**) surface morphology of samples at 1273 K for 180 h; (**b**) the weight gain curves at 1273 K and 1173 K.

The X-ray curves of the oxidation samples at 1173 K are shown in Figure 2. The Al oxide, Cr oxide and Ti oxide have been identified and detected after 1 h. The precipitation phase of NiTi was formed after 360 h. The intensities of those oxides increase with time. Otherwise, the matrix phase of $Al_{0.2}Co_{1.5}CrFeNi_{1.5}Ti_{0.3}$ HEA is FCC solid solution, and the peaks are detectable in 100 h. However, those oxide layers are too thick and hide the matrix FCC phase after 360 h.

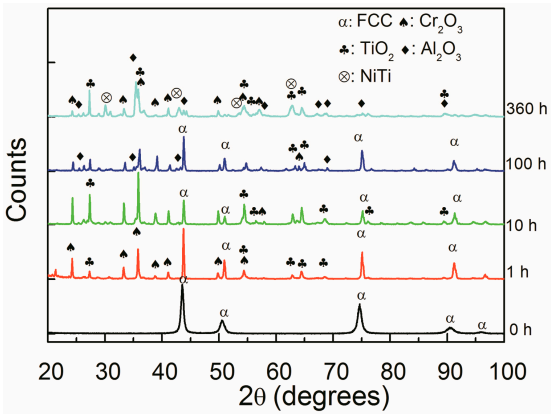

Figure 2. The X-ray curves of isothermal oxidation $Al_{0.2}Co_{1.5}CrFeNi_{1.5}Ti_{0.3}$ alloys at 1173 K for various times.

The microstructural evolution of the oxide sample is further observed. The microstructures of oxidation layers at 1173 K are shown in Figure 3. The thin and different oxide layers formed after 1 h, and the oxide layers are Ti oxide, Cr oxide, and Al oxide from the surface in sequence. As it is heating for 10 h, the oxide layer became thicker and grew in the deeper area. The thickness of the Ti oxide layer was almost unchanged at the surface, but it formed an NiTi-rich layer beneath the Cr oxide layer. However, the alumina layer is discontinuous, even lasting for 100 h, so only the Cr oxide layer is insufficient for the alloys to suffer at 1173 K or even a higher temperature. Therefore, the thickness of each oxide layer keeps growing, and the interdiffusion area is over 100 μm in Figure 3d after heating for 360 h. By the EDS mapping results, three regions, the Al-rich, the Ti-rich, and the Cr-rich regions, are compared in Figure 4. The total thickness of the reaction layer is also shown. The oxidation and interdiffusion are both considered. The Cr-rich region is mainly the oxide layer, and it is clearly directed. The thickness is about 10 μm after 360 h. The Al-rich regions are divided into the oxidation area and interdiffusion area. The alumina formed a porous and discontinuous layer, and dispersed close to the surface. Because of the depletion of Al, the NiTi compound phase is formed and that enlarges the Ti-rich region in Figure 3d [8].

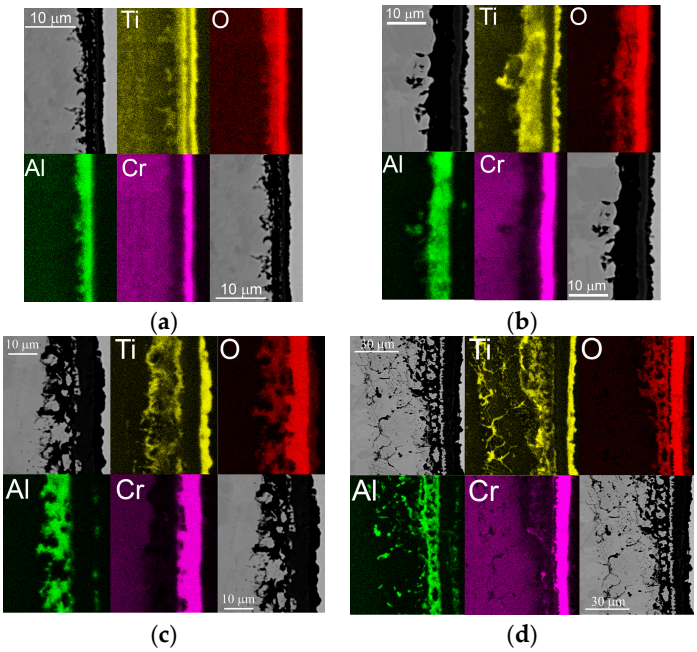

Figure 3. SEM-EDS mapping of isothermal oxidation samples at 1173 K for various times: (**a**) 1 h; (**b**) 10 h; (**c**) 100 h; and (**d**) 360 h.

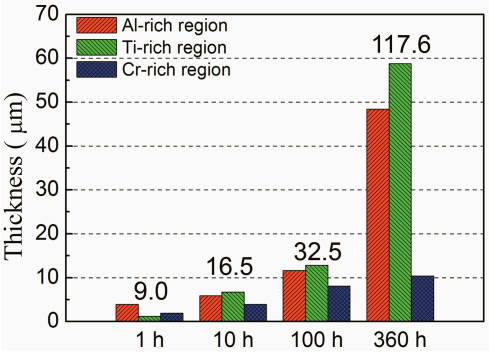

Figure 4. The thicknesses of the oxidation and interdiffusion layer are shown after the isothermal test. The numbers on the figure are the summation of these three regions.

3.2. Microstucture of Aluminizing Layers

There is generally Al coating and a IDZ (interdiffusion zone) with aluminization, and the present alloy also shows a similar structure in Figure 5. In this study, the aluminizing layer and interdiffusion zone are 50 μm and 18.3 μm respectively under 1273 K for 5 h. The other one is 71.3 μm and 24.6 μm respectively under 1323 K for 5 h. The composition of the aluminizing layers is almost the same, and it reveals that the temperature of 1273 K is good to fulfill the aluminization. The surface morphology and EDS mapping are shown in Figure 6. The aluminizing layer is uniform at the surface. From the EDS mapping results, Ti-rich particles that are less than 3 μm are distributed in the aluminizing layer. There are two areas in the IDZ region. One is rich in Co, Ni, and Ti, and the other is rich in Fe and Cr. Figure 7 shows the X-ray curve of the aluminization layer at 1273 K. Al(CoCrFeNiTi) is the main phase. Al_3Ti, Al_3Ni and NiTi are the minor phases.

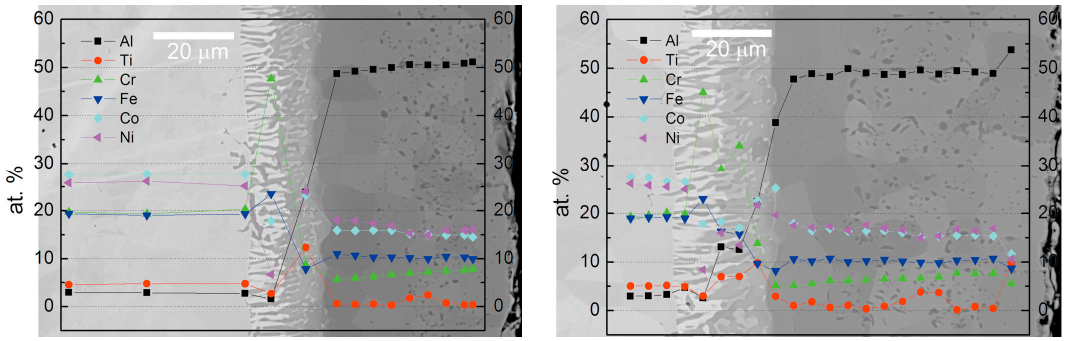

Figure 5. The microstructure of the aluminizing layer is shown, and the compositional profiles of each element are also inserted after the aluminizing process composition at (**a**) 1273 K and (**b**) 1323 K.

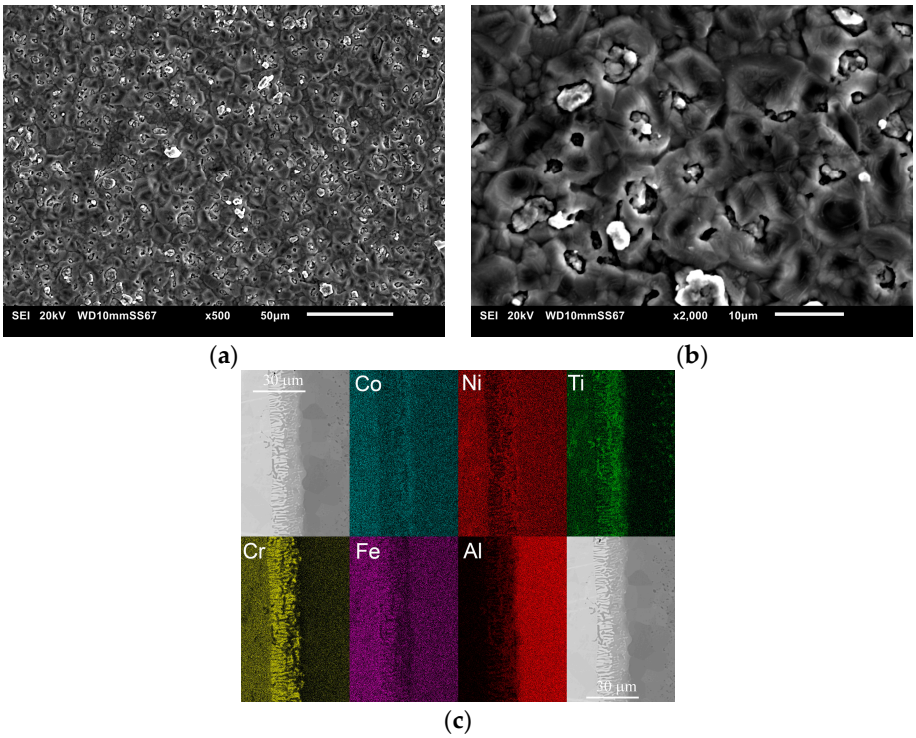

Figure 6. (**a**,**b**) The surface morphology after aluminizing coating at 1273 K; (**c**) the EDS mapping of each element by cross-section.

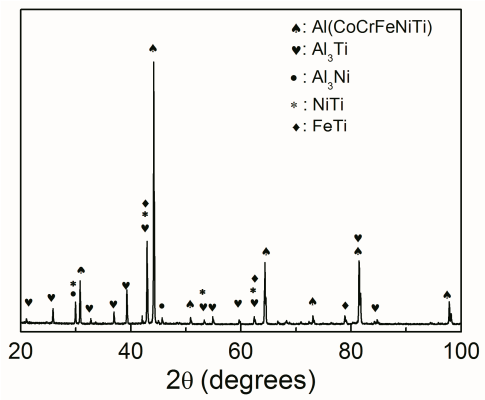

Figure 7. The X-ray curve of the aluminization layer at 1273 K.

3.3. Isothermal Oxidation with Aluminizing on HEA

Figure 8 shows the isothermal oxidation resistance of the $Al_{0.2}Co_{1.5}CrFeNi_{1.5}Ti_{0.3}$ HEA with aluminizing coating by aluminization at 1273 K for 5 h. The curve of the weight gain is almost the same at 1173 K, and the oxidation resistance of HEAs has improved obviously after aluminization compared to that without aluminization in Figure 1. As the temperature increases to 1273 K, the curve is flat before 200 h. However, the weight gain reduced a little between 200 h and 441 h; it is still sustained at 1273 K. The samples (refer to Supplementary Information) demonstrate that the aluminizing coating on HEAs is still good to protect the substrate after 441 h at 1173 K and 1273 K. When testing at 1373 K, the curve is shown to decrease with a wavy motion, because the coating layer is affected by both oxidation and spallation.

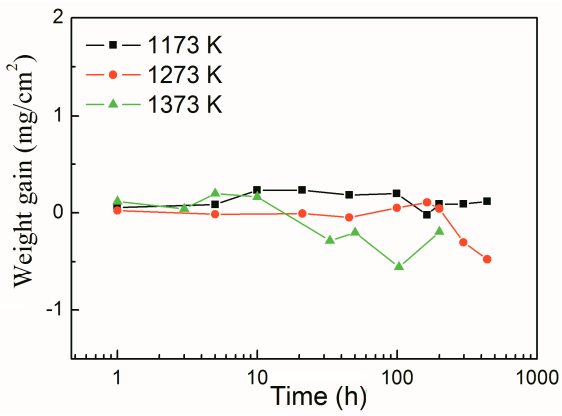

Figure 8. The isothermal oxidation resistance of the $Al_{0.2}Co_{1.5}CrFeNi_{1.5}Ti_{0.3}$ alloy after aluminizing at 1173 K, 1273 K and 1373 K.

4. Discussion

For oxidation results in the present HEA, the Ti oxide formed the fastest at the surface; however, its growth rate is inhibited by the Cr oxide layer. The limited Al molar ratio leads to the non-continuous alumina beneath the Cr oxide layer, so the Cr oxide layer is growing with time in Figure 3b,d. Therefore, the FCC $Al_{0.2}Co_{1.5}CrFeNi_{1.5}Ti_{0.3}$ HEA starts to precipitate the NiTi-rich phase because it lacks Al. For the $Co_{1.5}CrFeNi_{1.5}Ti_{0.5}$ HEA, it possess mainly a FCC structure; the η phase (Ni_3Ti) is at the interdendritic region in the as-cast condition which is stable between 1073 K and 1273 K. By the directional solidification process, it is found that Co, Cr, and Fe partition toward the dendritic region, while Ni and Ti partition toward the interdendritic areas [8]. That reveals a similar tendency in this

study. As the aluminum diffused to the surface, the composition of the matrix will be close to that of $Co_{1.5}CrFeNi_{1.5}Ti_{0.5}$.

By aluminization, the Al coating is stable and contains Al at about 50 at %. In the interdiffusion zone (IDZ), one region is rich in Co, Ti, and Ni, since they have high mixing enthalpy with Al. As Al just diffuses to the interface during aluminization, the diffusivity of Co, Ti and Ni is promoted. Therefore, the other region, rich in Cr and Fe, is formed followed by the previous region in Figure 6c. However, the Al is continuously diffused and reached a stable concentration with the other elements for a longer time. At the same time, Ti diffused from the matrix into the coating layers and formed the second phase. Its structure and composition need further study. In Figures 5 and 7, the coating layer contains the Al(CoCrFeNiTi) phase and Ti-rich phase. As the alumina forms at the surface at high temperature, the high entropy effect will stabilize the aluminizing layer. By the formation of the coating layer in Figure 6, the reverse reaction can be inferenced. If the dense and continuous alumina were formed at the surface, the IDZ close to the matrix may transform to the matrix phase again at a temperature over 1273 K. At the moment, the concentration of the aluminum is decreased, and the Ti-rich phase will be dissolved again. It is close to the matrix phase of $Al_{0.2}Co_{1.5}CrFeNi_{1.5}Ti_{0.3}$.

Comparing to Figures 1 and 8, the oxidation resistance of aluminizing $Al_{0.2}Co_{1.5}CrFeNi_{1.5}Ti_{0.3}$ is improved and can be sustained at 1273 K, lasting for 441 h without spallation. It is believed that the coating is covered with alumina at the surface, and is comparable to the substrate at the interface. However, the curve of the isothermal oxidation at 1373 is slightly unstable, but much better than that of HEAs without aluminization. The microstructures of these aluminizing samples after isothermal testing need further observation. The cyclic oxidation test is also worth studying in the future.

5. Conclusions

Aluminization by packing cementation, which is a popular industrial process, is suitable for FCC solid solution phase $Al_{0.2}Co_{1.5}CrFeNi_{1.5}Ti_{0.3}$ HEA. The aluminizing coating layer of 50 μm can be formed at 1273 K for 5 h, and it enhances the oxidation resistance up to 1273 K at least. The phases of the coating layer are Al(CoCrFeNiTi) and a Ti-rich phase. It contributes to the favorable oxidation resistance of the present alloys. Therefore, the alumina is good for surface stability, and the high entropy effect in HEAs further stabilizes the interface between the coating and substrate at high temperature.

Supplementary Materials: The following are available online at www.mdpi.com/1099-4300/18/10/376/s1, Figure S1: The isothermal oxidation resistance of the $Al_{0.2}Co_{1.5}CrFeNi_{1.5}Ti_{0.3}$ alloy after aluminizing: the surface morphology samples at (a) 1173 K for 200 h and 441 h; and (b) 1273 K for 195 h and 441 h.

Acknowledgments: The authors would like to thank the financial support from Ministry of Science and Technology, Taiwan, project grant number: 104-2218-E-007-017. Che-Wei Tsai would like to thank Murakami for discussion on the aluminization of HEAs and for supporting his stay at NIMS in Japan.

Author Contributions: Che-Wei Tsai and Kzauki Kasai conceived and designed the experiments; Hideyuki Murakami performed the experiments; Che-Wei Tsai and Kuen-Cheng Sung analyzed the data; Che-Wei Tsai wrote the paper. All authors commented on the manuscript at all stages. All authors have read and approved the final manuscript.

Conflicts of Interest: The authors declare no conflict of interest.

References

1. Yeh, J.W.; Chen, S.K.; Lin, S.J.; Gan, J.Y.; Chin, T.S.; Shun, T.T.; Tsau, C.H.; Chang, S.Y. Nanostructured high-entropy alloys with multiple principal elements: Novel alloy design concepts and outcomes. *Adv. Eng. Mater.* **2004**, *6*, 299–303. [CrossRef]
2. Yeh, J.W. Recent progress in high-entropy alloys. *Ann. Chim. Sci. Mater.* **2006**, *31*, 633–648. [CrossRef]
3. Zhang, K.B.; Fu, Z.Y.; Zhang, J.Y.; Wang, W.M.; Wang, H.; Wang, Y.C.; Zhang, Q.J.; Shi, J. Microstructure and mechanical properties of $CoCrFeNiTiAl_x$ high-entropy alloys. *Mater. Sci. Eng. A Struct. Mater.* **2009**, *508*, 214–219. [CrossRef]

4. Zhang, K.B.; Fu, Z.Y.; Zhang, J.Y.; Wang, W.M.; Lee, S.W.; Niihara, K. Characterization of nanocrystalline CoCrFeNiTiAl high-entropy solid solution processed by mechanical alloying. *J. Alloys Compd.* **2010**, *495*, 33–38. [CrossRef]
5. Zhang, K.B.; Fu, Z.Y. Effects of annealing treatment on properties of CoCrFeNiTiAlx multi-component alloys. *Intermetallics* **2012**, *28*, 34–39. [CrossRef]
6. Zhang, K.B.; Fu, Z.Y. Effects of annealing treatment on phase composition and microstructure of CoCrFeNiTiAlx high-entropy alloys. *Intermetallics* **2012**, *22*, 24–32. [CrossRef]
7. Chuang, M.H.; Tsai, M.H.; Wang, W.R.; Lin, S.J.; Yeh, J.W. Microstructure and wear behavior of $Al_xCo_{1.5}CrFeNi_{1.5}Ti_y$ high-entropy alloys. *Acta Mater.* **2011**, *59*, 6308–6317. [CrossRef]
8. Yeh, A.C.; Chang, Y.J.; Tsai, C.W.; Wang, Y.C.; Yeh, J.W.; Kuo, C.M. On the Solidification and Phase Stability of a Co-Cr-Fe-Ni-Ti High-Entropy Alloy. *Metall. Mater. Trans. A Phys. Metall. Mater. Sci.* **2014**, *45*, 184–190. [CrossRef]
9. Chang, Y.J.; Yeh, A.C. The evolution of microstructures and high temperature properties of $Al_xCo_{1.5}CrFeNi_{1.5}Ti_y$ high entropy alloys. *J. Alloys Compd.* **2015**, *653*, 379–385. [CrossRef]
10. Wollner, S.; Zaefferer, S.; Goken, M.; Mack, T.; Glatzel, U. Characterization of phases of aluminized nickel base superalloys. *Surf. Coat. Technol.* **2003**, *167*, 83–96. [CrossRef]
11. Li, H.X.; Qiao, M.; Zhou, C.G. Formation and cyclic oxidation resistance of Hf-Co-modified aluminide coatings on nickel base superalloys. *Mater. Chem. Phys.* **2014**, *143*, 915–920. [CrossRef]
12. Kasai, K.; Murakami, H.; Kuroda, S.; Imai, H. Effect of Surface Treatment and Crystal Orientation on Microstructural Changes in Aluminized Ni-Based Single-Crystal Superalloy. *Mater. Trans.* **2011**, *52*, 1768–1772. [CrossRef]
13. Kasai, K.; Murakami, H.; Noda, K. Effect of Thermal History on Microstructural Changes in Aluminized Nickel-Based Single-Crystal Superalloy. *Mater. Trans.* **2013**, *54*, 2252–2257. [CrossRef]
14. Murakami, H.; Sakai, T. Anisotropy of secondary reaction zone formation in aluminized Ni-based single-crystal superalloys. *Scr. Mater.* **2008**, *59*, 428–431. [CrossRef]